Biophysical Journal Volume 65 September 1993 985–991

Evidence for a γ-Turn Motif in Antifreeze Glycopeptides

Joel A. Drewes and Kathy L. Rowlen
Department of Chemistry and Biochemistry, University of Colorado, Boulder, Colorado 80309 USA

ABSTRACT Knowledge of the secondary structure of antifreeze peptides (AFPs) and glycopeptides (AFGPs) is crucial to understanding the mechanism by which these molecules inhibit ice crystal growth. A polyproline type II helix is perhaps the most widely accepted conformation for active AFGPs; however, random coil and α-helix conformations have also been proposed. In this report we present vibrational spectroscopic evidence that the conformation of AFGPs in solution is not random, not α-helical, and not polyproline type II. Comparison of AFGP amide vibrational frequencies with those observed and calculated for β and γ-turns in other peptides strongly suggests that AFGPs contain substantial turn structure. Computer-generated molecular models were utilized to compare γ-turn, β-turn, and polyproline II structures. The γ-turn motif is consistent with observed amide frequencies and results in a molecule with planar symmetry with respect to the disaccharides. This intriguing conformation may provide new insight into the unusual properties of AFGPs.

INTRODUCTION

In 1969 DeVries and Wohlschlag demonstrated that the noncolligative freezing point depression observed for blood from Antarctic fish was due to glycopeptides. These "antifreeze" glycopeptides (AFGPs) consist of a group of eight closely related molecules ranging in molecular mass from 2600 to 33,000 Da (DeVries, 1971). The most active AFGPs, in terms of ice crystal growth inhibition, are those in the molecular mass range of 20,000–33,000 Da (Burcham, 1984). These active AFGPs have the same basic repeat unit of Ala-Thr-Ala with a disaccharide, β-D-galactopyranosyl(1→3)-2-acetamido-2-deoxy-α-D-galactopyranose (Gal(β1–3)-αGalNAc), *O*-glycosidically linked to each threonyl side chain (DeVries, 1971).

In addition to AFGPs there are three known types of antifreeze peptides (AFPs) (Davies, 1990). Yang et al. found the crystal structure of one AFP (37-mer) to be a single α-helix (Yang, 1988). This evidence, in conjunction with the observation that both AFPs and AFGPs adsorb to ice surfaces (Raymond, 1977), led to the postulate that antifreeze activity derives from an alteration of the ice surface by AFP adsorption (DeVries, 1984; Knight, 1991). Knight et al. demonstrated that AFPs selectively adsorb to either the pyramidal or prism planes of ice (Knight, 1991). The authors suggested that the AFPs were aligned such that the lattice spacing on a particular ice plane matched the spacing of polar residues on the AFP. For a molecule that has a "hydrophobic side" and a "hydrophilic side," the most widely accepted mechanism for ice crystal growth inhibition involves adsorption of the hydrophilic side of the molecule to the ice surface, which, in turn, results in exposure of the hydrophobic side to solution. In essence, ice crystal growth is prevented by hydrophobic exclusion of water molecules from the crystal surface.

Since direct determination of the conformation of antifreeze molecules at the ice-water interface remains a challenging experimental problem, the first step in testing the postulated antifreeze mechanism with respect to AFGPs is to understand their solution-phase secondary structure. While circular dichroism (CD, Bush, 1981), nuclear magnetic resonance (NMR, Berman, 1980; Bush, 1984, 1986), and Raman (Tomimatsu, 1976) spectroscopic techniques have all been applied to the problem, the question of AFGP secondary structure remains unresolved. A polyproline type II helix is perhaps the most widely accepted conformation for active AFGPs (Bush, 1981, 1984, 1986; Berman, 1980; Homans, 1985); however, random coil (Berman, 1980) and α-helix (Tomimatsu, 1976) conformations have also been proposed. In this report we present evidence that the conformation of AFGPs in solution is not random, not α-helical, and not polyproline type II. Based on comparison with calculated frequencies for γ-turns, as well as molecular modeling, a γ-turn motif is proposed as a plausible conformation for active AFGPs.

MATERIALS AND METHODS

Raman

The Raman instrument is comprised of an air-cooled Ar^+ laser (ILT, Salt Lake City, UT), premonochromator (Optometrics TGF-302, Ayer, MA), half-wave plate (Melles Griot, Irvine, CA), 40-cm focal length lens (JML, Rochester, NY), custom built temperature controlled sample stage, f/1.7 collection lens, holographic edge filter (Physical Optics Corp.), f/4 focusing lens, a single 0.5-m f/4 spectrograph with 1200 grooves/mm grating (Spex 500 M, Edison, NJ), and a liquid nitrogen-cooled charge-coupled device (CCD, Princeton Instruments, Trenton, NJ). For room temperature studies a capillary, with 90° collection optics, was used as the sample cell. The use of a Raman holographic edge filter readily allows for measurements within 100 cm^{-1} of the Rayleigh line. The use of a CCD and the 488-nm line from the laser provides snapshots of spectral regions covering ~900 cm^{-1}. Polarization from the Ar^+ laser is specified at 100:1; qualitative polarization studies were conducted by rotating the plane of polarization for incident light, i.e., fixed collection. Qualitative polarization measurements can be made in the absence of a polarization scrambler by insuring that the monochromator setting is not varied between the two experiments. Calibration of the signal in wavenumbers (cm^{-1}) is based on a third-order polynomial fit

Received for publication 24 February 1993 and in final form 21 May 1993.
Address reprint requests to Kathy L. Rowlen at the Department of Chemistry and Biochemistry, University of Colorado, Campus Box 215, Boulder, CO 80309.

0006-3495/93/09/985/07 $2.00

to the spectrum of indene (Aldrich Chemical Co., Milwaukee, WI, 98%). The standard error in band position is conservatively estimated to be ± 2 cm^{-1}. The temperature of the sample stage was controlled with a NesLab RTE 110 circulator. An Omega multimeter equipped with a calibrated K-type thermocouple was used to determine the temperature of the sample.

The samples were obtained from A. L. DeVries of the University of Illinois at Champaign-Urbana; the purification process was described earlier (DeVries, 1970). AFGP 1–4 solutions were made 10% by weight (~5 mM) in H_2O, D_2O (99.9% Cambridge Isotope Laboratories, Woburn, MA), and dimethyl sulfoxide (DMSO) (99.9% Mallinckrodt). *N*-Acetyl-D-galactosamine (Sigma Chemical Co., St. Louis, MO, 98%) was used as purchased.

Infrared

A Perkin-Elmer 1600 series FTIR was used to obtain the spectrum of AFGP 1–4. Solid pellet samples of AFGP 1–4 were pressed at 20% by weight in KBr. Silver bromide windows (Spectra Tech. Inc.) were used for aqueous studies.

Molecular Model

Insight II (version 2.1.0) on a silicon graphics workstation was used to construct the molecular models. The procedure for constructing each was as follows: 1) individual residues were extracted from a data base, 2) dihedral angles were imposed sequentially, and 3) the secondary structure was checked to insure that no two atoms were closer than allowed van der Waals distances.

RESULTS AND DISCUSSION

Vibrational studies of biological molecules have firmly established the sensitivity of amide transitions to secondary structure (Krimm, 1986, 1987; Carey, 1982). In this report, both Raman and infrared studies of AFGP 1–4 are presented. Raman spectral assignments are based on dipeptide spectra (Ala-Ala, Ala-Thr, and Thr-Ala), isotope substitution (D_2O), polarization, and solvent studies, as well as reference to literature assignments (Tomimatsu, 1976; Krimm, 1986, 1987; Carey, 1982).

Amide I

The amide I transition, which is a combination of C=O stretch, C-N out-of-phase stretch and $C^{\alpha}CN$ deformation, can range from 1620 to 1700 cm^{-1}. Fig. 1 shows the Raman spectrum of AFGP 1–4 in H_2O at 25°C. In Fig. 2 the Raman spectra of AFGP 1–4 in H_2O and D_2O are shown over the critical region of 1000–1700 cm^{-1}. These spectra were obtained under exactly the same conditions, i.e., equal concentrations, the same temperature, and the same monochromator setting. Since our instrument avoids the necessity of wavelength scanning and no splicing was required for this wavenumber range, the relative band positions in H_2O and D_2O are very accurate. In both spectra, the solvent background was subtracted. For H_2O the background is due to the O-H bending mode which partially overlaps the amide I and amide II modes. In D_2O, after equilibrium is established, the background also contains contributions from O-H bend which must be subtracted accordingly. Table 1 is a summary of the measured band frequencies in H_2O. For comparative

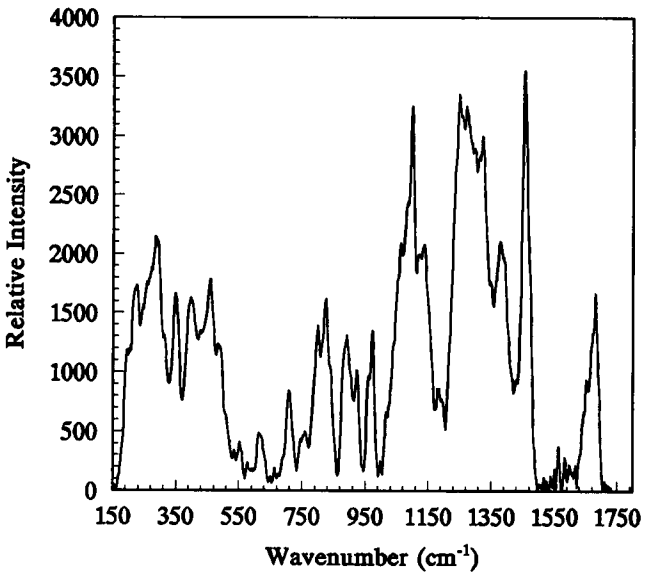

FIGURE 1 Raman spectrum AFGP 1–4 10% by weight in H_2O at 25°C. The spectrum was obtained with a 300-s integration time. The solvent background was substrated, and the data were smoothed with a 7-point Savitsky-Golay filter.

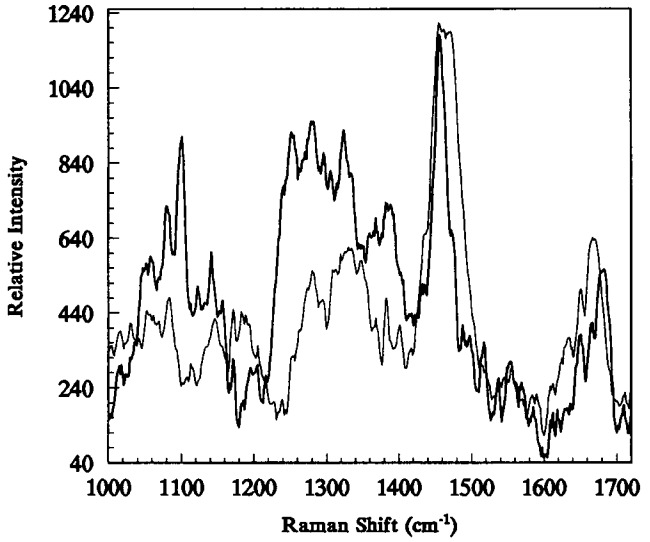

FIGURE 2 Raman spectrum (1000–1700 cm^{-1}) AFGP 1–4 10% by weight in H_2O (*darker line*) and D_2O at 25°C. Each spectrum was obtained by summing five spectra taken with a 40-s integration time. The solvent background was subtracted (see text for details), and the data smoothed with a 7-point Savitsky-Golay filter.

purposes, Table 1 also contains a summary of typical frequencies for "standard" secondary structures. For AFGP, the strong band at 1684 cm^{-1}, along with the bands at 1667 and 1648 cm^{-1} are attributed to peptide amide I modes. These bands appear to be substantially polarized, which may indicate a large contribution from the symmetrical C=O stretch. Based on the spectrum of *N*-acetyl-D-galactosamine, the band at 1638 cm^{-1} is assigned to the *N*-acetyl chromophore on the disaccharide.

TABLE 1 Frequencies for various secondary structures (1700–1000 cm^{-1})

AFGP 1–4			γ-Turn,	β-Turn		PP II,	α-Helix	
Raman	IR (aq)	(solid)	Calculated	Raman	IR	Raman	Raman	IR
1684		1684	1684	1741	1741	1642	1655	1658
1667		1670	1670	1689	1686			
1648		1653	1655	1674	1673			
1638*		1645	1653	1656	1655			
				1644	1639			
1586	1556	1554	1552		1568	1550		1545
1567	1541	1540	1529		1548			1516
1550		1523	1526		1525			
1538	1506	1508	1509					
1517								
1498						1473	1458	1458
1488						1457		
1457								
1333			1390	1333	1333	1354	1377	1381
1317			1367	1325		1306	1338	
1304				1316	1314	1275	1326	1328
1291			1336	1291	1294	1253	1308	1307
1277*			1327			1210	1278	
			1297			1197	1271	1270
			1282			1186	1261	1265
			1242			1170	1167	1170
			1225			1102	1105	1108
						1056	1050	1051
						1008	1017	1016

AFGP, The bands were taken from the unspliced data shown in Fig. 2, only bands that were reproducible over several data sets are reported. The bands with an asterisk are assigned to the disaccharide *N*-acetyl group. IR bands are from 10% by weight in H_2O and 20% by weight in KBr. **γ-turn**, calculated bands for CH_3-CO-(L-Ala)$_3$-NH-CH_3, (Krimm, 1986). **β-turn**, observed bands for Z-Gly-Pro-Leu-Gly-OH (Krimm, 1986). **PP II** = Polyproline II, ~16% by weight observed in H_2O at 25°C (Sigma, 98% M_r ~8000). **α-Helix**, observed for poly(L-Ala) (Krimm, 1986).

Referring to Table 1, the position of the amide I bands in AFGP 1–4 correlates well with the predicted range (1650–1685 cm^{-1}) for amide I modes in γ-turns (Krimm, 1986). Krimm and Bandekar (1986) note that, for helical conformations in solution, the amide I mode is strong and usually appears as a single band near 1652 cm^{-1}. A comparison of bands listed in Table 1 indicates that there is little, if any, α-helical structure in AFGPs, contrary to the conclusion of the previous Raman study (Tomimatsu, 1976). As additional evidence, the strongest amide I band in AFGP shifts 20 cm^{-1} to lower frequency upon deuteration, from 1684 cm^{-1} in H_2O to 1664 cm^{-1} in D_2O. This shift is much larger than the amide I (containing NH_2 contributions) shift observed for most helices (8–10 cm^{-1}) and β-sheets (5 cm^{-1}); however, the amide I region of β-turns can downshift 14 cm^{-1} or more upon deuteration (Krimm, 1986, 1987). The primary indication that the AFGP amide I modes are not due to β-turn structure is the absence of bands above 1700 cm^{-1}. Note that in Fig. 2 the apparent weak band at 1710 cm^{-1} is not reproducible and is attributed to noise enhancement from background subtraction. The position of the AFGP amide I band at 1691 cm^{-1} in DMSO (in which AFGP aggregates and eventually precipitates) and in the solid phase also correlates well with the amide I position of turn structures in the solid or crystalline phase (Krimm, 1986).

The most widely accepted conformation for AFGPs is a polyproline type II helix (Bush, 1981, 1984, 1986; Homans, 1985). However, the Raman spectrum of commercially obtained polyproline type II (Sigma, 98%) was determined using exactly the same experimental conditions as for AFGP, and few spectral similarities were observed (see Fig. 3). Most notable is the lack of shift in the polyproline II amide I region upon deuteration; the band shifts from 1642 cm^{-1} in H_2O to

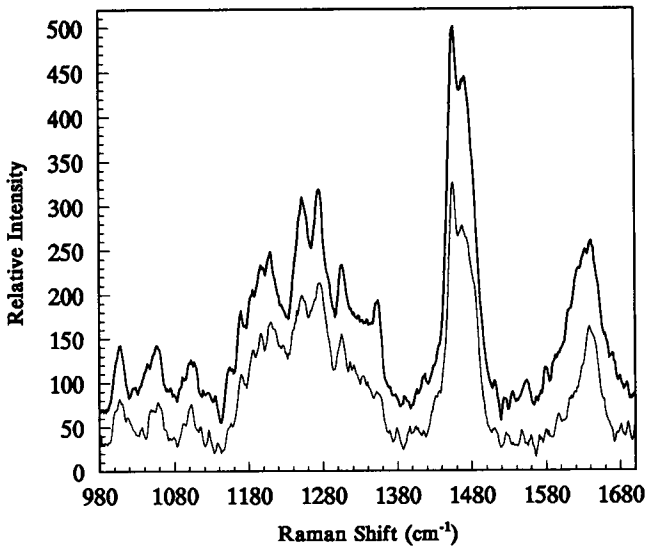

FIGURE 3 Raman spectrum of 16% by weight polyproline II in H_2O (*darker line*) and D_2O. The spectra were each taken with a 50-s integration time at 25°C and were smoothed with a 7-point Savitsky-Golay filter.

1639 cm^{-1} in D_2O, only 3 cm^{-1}. The absence of large frequency shifts in polyproline is due, in part, to the lack of exchangeable amide protons. However, the small shift also implies that there is little change in the hydrogen-bond environment of C=O. In polyproline II there is no intramolecular hydrogen bond stabilization; this is obviously different than the case for AFGP. Thus, the amide I region, for both native and perturbed states, provides evidence that the secondary structure of AFGP in solution is not a polyproline type II structure. We will build on this evidence by analysis of the entire spectrum.

Amide II

The amide II mode, which is usually weak in Raman scattering but can be distinguished in infrared absorption, has contributions from N—H in-plane bend, C—N stretch, and C=O in-plane bend. The amide II region is typically located within the 1500–1600-cm^{-1} range. Carbohydrates do not exhibit any bands in this region (Vasko, 1972). Fig. 4 shows the solid infrared spectrum of AFGP 1–4 in KBr. The IR bands observed at 1554, 1540, 1523, and 1508 cm^{-1} in AFGP are attributed to amide II modes. While there are Raman amide II bands reported in Table 1, these weak bands are suspect due to spectral interference from H_2O. Note that AFGP band positions in the amide II region compare well with the positions of calculated amide II bands in γ-turn structures (Krimm, 1986). There also appears to be reasonable agreement with β-turn structure. Polyglycine II, which has a proposed polyproline II helical structure and exhibits intramolecular hydrogen bonding, has only one amide II band centered at 1550 cm^{-1} (Krimm, 1987).

Amide III

The amide III region (1200–1400 cm^{-1}) consists primarily of N-H in-plane bend and C-N stretch. The bands at 1333, 1317, 1304, and 1291 cm^{-1} are attributed to the backbone amide III modes. All of these bands occur above 1290 cm^{-1}, which is considered to be characteristic of turns (Krimm, 1986). In general, α-helix and β-sheet structures do not exhibit amide III frequencies above 1290 cm^{-1} (Krimm, 1986; Van Wart, 1978). Again, referring to Table 1, it is obvious that the amide III modes of polyproline II do not correspond to those observed for AFGP. However, there is considerable correlation between the amide III bands for β-turns and those of AFGP.

Temperature dependence

A Raman spectroscopic temperature study of AFGP 1–4 over the range of −6°C (frozen) to 68°C shows no changes in band positions or intensities (within experimental error), as shown

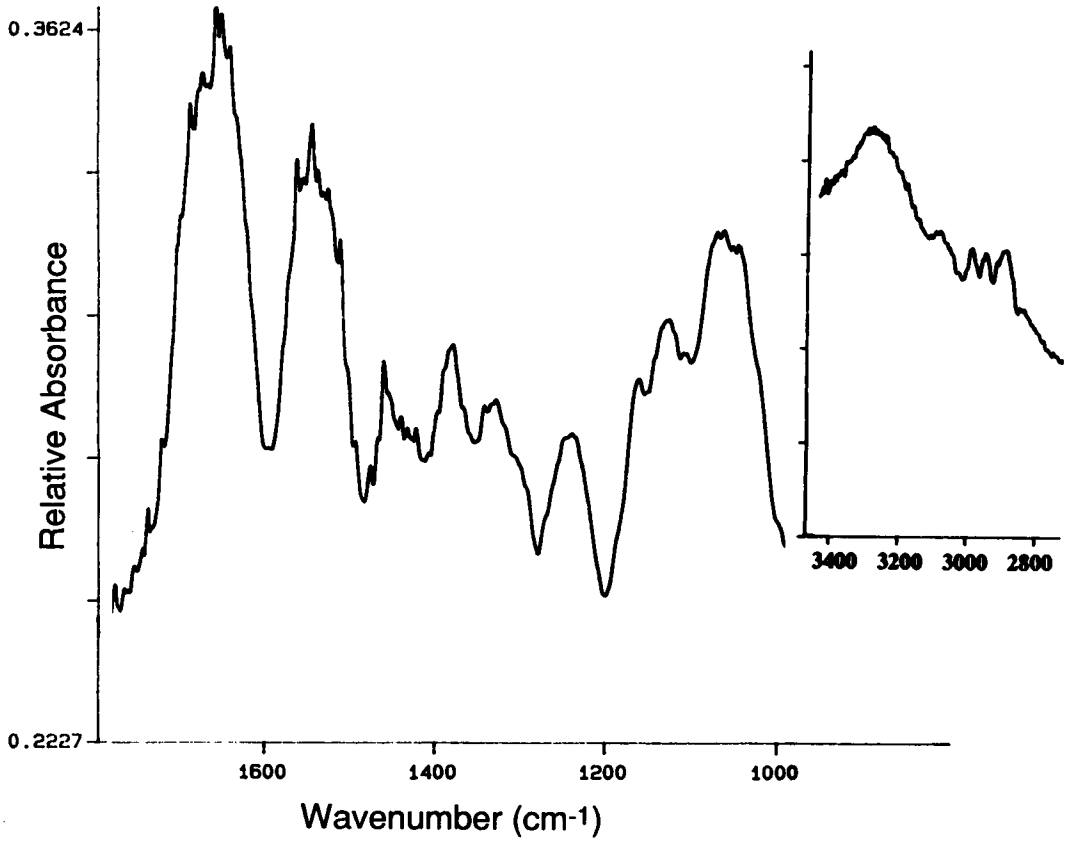

FIGURE 4 Infrared absorption spectrum of AFGP 1–4 20% by weight in KBr (~25°C). The amide A region is shown in the inset. From 16 scans at 4-cm^{-1} resolution.

in Fig. 5. Above 70°C the glycopeptide aggregates and eventually precipitates from solution. The lack of temperature dependence was also noted in the Raman study conducted by Tomimatsu et al. (1976). The fact that the vibrational spectrum does not exhibit a discernible temperature dependence suggests that either the secondary structure is quite stable or that there is no secondary structure. Indeed, the CD spectrum of AFGP 1–4 (Bush, 1981) is qualitatively similar to that of a random coil (Johnson, 1990). However, diffusion coefficient measurements of AFGP indicate that the structure cannot be a true random coil (Ahmed, 1975). NMR studies both reject (Berman, 1980) and support the idea that AFGP 1–4 has some degree of secondary structure (Bush, 1984, 1986; Homans, 1985).

Denaturation

In order to further test the existence of secondary structure in AFGP 1–4, urea was used to denature the glycopeptide. The changes observed in the Raman spectrum of AFGP 1–4 in 10 M urea are comparable in magnitude to the Raman spectroscopic changes observed between native and denatured ribonuclease A (Carey, 1982). Specifically, the amide I region shifts to a higher frequency, a low amplitude band emerges on the high frequency side of the CH_3 deformation region, and significant changes in relative intensity are observed in the amide III and skeletal (1000–1200 cm^{-1}) regions. While the Raman spectroscopic differences are not drastic, they do imply a change in secondary structure. The significant changes observed in the Raman spectrum upon deuteration also indicate a change in secondary structure (discussed in greater detail below).

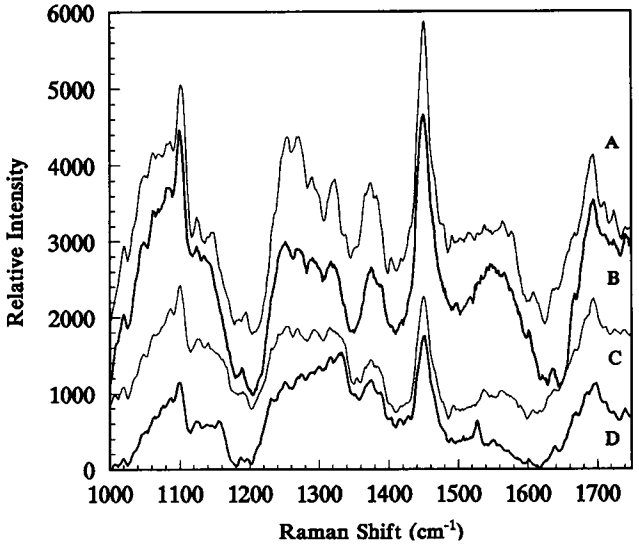

FIGURE 5 Raman spectrum of AFGP 1–4 (20% by weight in H_2O) as a function of temperature. The temperatures for A, B, C, and D are frozen (~–6°C), 22, 41, and 68°C, respectively. The spectra were taken with a 140-s integration time, and were smoothed with a 7-point Savitsky-Golay filter. At 68°C AFGP begins to denature. The water background is incompletely subtracted in these spectra.

Amide A

It is proposed that the unusual stability of AFGP 1–4 arises from a combination of intramolecular forces, i.e., both hydrophobic (dominant at high temperatures) and hydrogen bond (dominant at lower temperatures) interactions (Murphy, 1990). A γ-turn structure would provide both stabilizing forces. The postulated existence of intramolecular hydrogen bond stabilization is supported by the width of the amide A and amide II regions; the amide A region for AFGP 1–4 in KBr ranges from 3200 to 3400 cm^{-1} (see Fig. 4). Based on a correlation between hydrogen bond length (as determined by crystallography) and the range of amide A frequencies (Krimm, 1986), it appears that N · · · O bond distances in AFGP 1–4 range from 2.65 to 2.95 Å, which, in turn, suggests that the amide NH is hydrogen-bonded in a distribution of environments. For example, within a γ-turn structure some residues would form intramolecular N—H · · · O hydrogen bonds, whereas other residues would form solvent N—H · · · O hydrogen bonds.[1] The disaccharide NH is expected to be more exposed than backbone NH groups and may therefore have a slightly different average H-bond length. The width of the amide II region, which contains an $NH_{(ib)}$ component, is also consistent with this interpretation (Krimm, 1986).

Hydrophobic interaction (the 1400 cm^{-1} and CH stretch regions)

Vibrational evidence for intramolecular hydrophobic interaction is based on the CH_3 deformation mode observed at 1459 cm^{-1} in the Raman spectrum. This band, in both H_2O and D_2O, was fit as the sum of three Gaussians (minimization of the sum of squares). In H_2O, the band width (sum of the full width at half maximum for all three Gaussians) is 17 cm^{-1}.[2] In D_2O, at the same concentration and temperature, the band width is 39 cm^{-1}; an increase of 22 cm^{-1}. This broadening of the CH_3 deformation mode in D_2O strongly indicates hydrophobic (e.g., methyl-methyl) interactions (Hallén, 1986). Upon deuteration, the band at 1472 cm^{-1} evolves from a relatively weak mode in H_2O into a dominant mode. These trends may indicate enhanced differences in methyl group environments. For example, methyl groups within the pocket of a γ-turn might experience increased interactions in D_2O, whereas methyl groups exposed to the solvent would be expected to exhibit negligible differences. The increase in methyl group interaction within the pocket of a γ-turn may be explained by a stronger hydrogen bond upon deuteration (C=O · · · DN). Further evidence for a tightening of the γ-turn pocket may be found in the C—H stretch region. There are three Raman AFGP bands; 2991,

[1] AFGP binds a significant amount of water in its solid state.

[2] The band width of AFGP *1–4* in ice at –6°C is in agreement with the band width for AFGP *4* at –4°C (22 cm^{-1}) reported previously (Tomimatsu, 1976); thus, the distribution in chain lengths does not appreciably affect the band width.

2945, and 2891 cm^{-1} (IR solid 2980, 2942, 2881 cm^{-1}). The strongest band 2945 cm^{-1} is polarized and is thus attributed to the symmetrical C-H stretch. Upon deuteration, the band at 2891 cm^{-1} shifts to higher frequency and merges with the 2945 cm^{-1} band. *N*-Methyl acetamide in H_2O also exhibits three bands of similar frequency and relative intensity. No shift in frequency upon deuteration is observed for the corresponding C-H stretch of *N*-methyl acetamide (in D_2O). Thus, for AFGP, the shift in frequency is probably not due to direct interaction with the solvent, but may be the result of a slight conformational change. One may argue that the stronger CO · · · DN hydrogen bond would result in a tighter turn and therefore an increase in methyl-methyl interactions within the turn.

Concentration dependence

Due to the insensitivity of Raman spectroscopy, as well as fluorescent spectral interference, the dynamic range available for concentration studies is quite limited. The Raman spectrum (1000–1700 cm^{-1}) of AFGP 1–4 was investigated over a small concentration range: 30, 20, 10, and 5% by weight. Although no changes were observed in the spectrum, the range is insufficient to allow any conclusion to be drawn.

β-Turn or γ-turn?

The vibrational spectrum of AFGP appears to indicate a turn motif. Indeed, energetic considerations suggest that the most likely point of attachment for saccharides on glycoproteins is at a β-turn (Bush, 1982; Duben, 1983). However, NMR appears to rule out a β-turn conformation for AFGP (Bush, 1986). In addition, the amide I region does not contain modes above 1700 cm^{-1}. While our data do not unequivocally rule out a β-turn structure, molecular models of β-turns presented no clear symmetry that might explain the unique antifreeze activity of AFGPs. Bush and Feeney (1986) used NMR and conformational energy calculations to determine the peptide angles (ϕ, ψ) for AFGP 1–4. Analysis of their data on a Ramachandran plot shows that γ-turns fall within the given range of predicted lowest energy conformations.

Molecular model

A molecular model of four repeat monomers (monomer = Ala-Thr-Ala) was constructed using the dihedral angles given by Krimm (1987) for a γ_m turn. Other γ type turns were constructed and gave similar results. As can be seen in Fig. 6, intramolecular hydrogen bonds occur for alternating NH groups within the turns; the structure is stabilized and there is a distribution of NH environments. However, it must be noted that the hydrogen bonds of γ-turns are expected to be nonlinear, and therefore would be exposed to the solvent to a greater extent than intramolecular hydrogen bonds within an α-helix (Pease, 1977). The nonlinearity of intramolecular hydrogen bonds within a γ-turn may explain the amide proton temperature dependence observed in the NMR spectrum of AFGP (Bush, 1986). The van der Waals radii for methyl

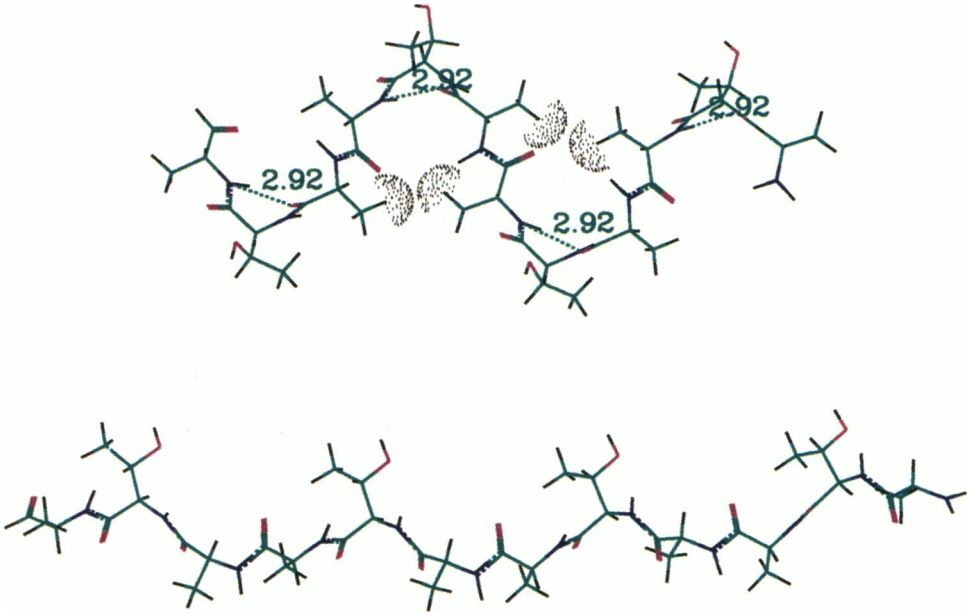

FIGURE 6 The top model is a γ_m structure constructed from four repeat units (4 × (Ala-Thr-Ala)). The dihedral angles were taken from Krimm and Bandekar (1986). In order to retain clarity, the disaccharides are not shown. Oxygen atoms are shown in red, hydrogen in black, nitrogen in purple, and carbon in green. The numbers represent the hydrogen bond distance as defined between nitrogen and oxygen. The van der Waal radii of four methyl hydrogens are designated with dots. All of the threonine hydroxyls are at the point of a turn. At the angle shown, all of the disaccharides would be oriented up toward the reader. The bottom model is the polyproline II conformation. The dihedral angles were taken from Bush and Feeney (1986). All of the disaccharides would be on the top side of the molecule, while the bottom side contains solvent-exposed methyl groups. While our data do not unequivocally rule out β-turn structure, as NMR apparently does (Bush, 1986), a model of an AFGP 4-mer constructed with β-turn (type 1) shows no distinct planar symmetry with respect the the disaccharides.

groups indicate possible hydrophobic interaction within the pocket of each turn, which is consistent with our interpretation of the Raman spectrum. A view through the molecular plane shows that all of the disaccharide linkages are on one side of the molecule. The spacing of the disaccharide side chains (as measured between threonyl hydroxyls) along the backbone in our model is twice the 4.5-Å spacing of alternate oxygen atoms on the prism faces in hexagonal ice. This type of spacing has been observed in AFPs and is thought to be associated with antifreeze activity (DeVries, 1984). Although the disaccharides have been omitted from the figure for clarity, this model clearly indicates the potential for interaction between the disaccharide and backbone.

For comparison, the polyproline II structure proposed by Bush and Feeney (1986) is also shown in Fig. 6. In this conformation all of the disaccharides are on one side of the molecule, as is true for the γ-turn model; however, the opposite side of the molecule is primarily hydrophobic, which is not true in the γ-turn model. All evidence currently available indicates that AFGPs do not undergo a significant conformational change upon adsorption to the ice surface. Both solution-phase structures shown in Fig. 6 offer an intuitive advantage over a completely random conformation, in that the molecule "pre-exists" in a conformation that allows maximum interaction between disaccharide hydroxyls and the ice surface. The intramolecular interactions found in the γ-turn structure may explain the extraordinary stability of AFGPs. By comparison, the polyproline II model for AFGPs shows little or no intramolecular stabilizing interactions[3] and has the energetically unfavorable condition of all alanine methyl groups exposed to solvent (Murphy, 1990; Hallén, 1986). The fact that the γ-turn structure does not have a solvent-exposed hydrophobic side may imply that the mechanism by which AFGPs inhibit ice crystal growth does not depend on hydrophobic repulsion of water from solution. That is, the adsorption of AFGPs to an ice surface by cooperative hydrogen boding over the length of a long peptide (the small AFGPs are not active in the absence of large AFGPs) may sufficiently alter the surface of an ice crystal, such that water molecules can no longer order at the surface in a manner that would promote crystal growth.

We thank Dr. Arthur L. DeVries for AFGP samples. K. L. Rowlen thanks the Beckman Foundation for a Young Investigator award.

REFERENCES

Ahmed, A. I., R. E. Feeney, D. T. Osuga, and Y. Yeh. 1975. Quasi-elastic light scattering studies of the hydrodynamic conformations of antifreeze glycoproteins. *J. Biol. Chem.* 250:3344–3347.

Berman, E., A. Allerhand, and A. L. DeVries. 1980. Natural abundance carbon 13 nuclear magnetic spectroscopy of antifreeze glycoproteins. *J. Biol. Chem.* 255:4407–4410.

Burcham, T. S., D. T. Osuga, M. J. Knauf, R. E. Feeney, and Y. Yeh. 1984. Antifreeze glycoproteins, and influence of polymer length, and ice crystal habit on activity. *Biopolymers.* 23:1379–1384.

Bush, C. A., R. E. Feeney, D. T. Osuga, S. Ralapati, and Y. Yeh, 1981. Antifreeze glycoprotein: conformational model based on vacuum ultraviolet circulaar dichroism. *Int. J. Peptide Protein Res.* 17:125–129.

Bush, C. A., S. Ralapati, G. M. Matson, R. B. Yamasaki, D. T. Osuga, Y. Yeh, and R. E. Feeney. 1984. Conformation of the antifreeze glycoprotein of polar fish. *Arch. Biochem. Biophys.* 232:624–631.

Bush, C. A., and R. E. Feeney. 1986. Conformation of the glycotripeptide repeating unit of antifreeze glycoprotein of polar fish as determined from the fully assigned proton n.m.r. *Int. J. Peptide Protein Res.* 28:386–397.

Bush, C. A. 1982. Conformational energy calculations on glycosylated turns in glycoproteins. *Biopolymers.* 21:535–545.

Carey, P. R. 1982. Biological Applications of Raman, and Resonance Raman Spectroscopies. Academic Press, New York. 80–84.

Davies, P. L., and C. L. Hew. 1990. Biochemistry of fish antifreeze proteins. *FASEB J.* 4:2460–2468.

De Vries, A. L., and D. E. Wohlshlag. 1969. Freezing resistance in some antarctic fishes. *Science.* 163:1073–1075.

DeVries, A. L., J. Vandenheede, and R. E. Feeney. 1971. Primary structure of freezing point-depressing glycoproteins. *J. Biol. Chem.* 246:305–308.

DeVries, A. L. 1984. Role of glycopeptides, and peptides in inhibition of crystallization of water in polar fishes. *Phil. Trans. R. Soc. Lond. B.* 304:575–587.

DeVries, A. L., S. K. Komatsu, and R. E. Feeney. 1970. Studies of the structure of freezing point-depressing glycoproteins from an Antarctic fish. *J. Biol. Chem.* 245:2901–2908.

Duben, A. J., and C. A. Bush. 1983. Monte Carlo calculations on the conformations of models for the glycopeptide linkage of glycoproteins. *Arch. Biochem. Biophys.* 225:1–15.

Hallén, D., S. O. Nilsson, W. Rothschild, and I. Wadsö. 1986. Enthalpies, and heat capacities for *n*-alkan-1-ols in H_2O, and D_2O. *J. Chem. Thermodyn.* 18:429–435.

Homans, S. W., A. L. DeVries, and S. B. Parker. 1985. Solution structure of antifreeze glycopeptides. *FEBS Lett.* 183:133–137.

Johnson, C. W. 1990. Protein secondary structure, and circular dichroism: a practical guide. *Proteins: Struct. Funct. Genet.* 7:205–214.

Knight, C. A., C. C. Cheng, and A. L. DeVries. 1991. Adsorption of α-helical antifreeze peptides on specific ice crystal surface planes. *Biophys. J.* 59: 409–418.

Krimm, S., and J. Bandekar. 1986. Vibrational spectroscopy, and conformation of peptides, polypeptides, and proteins. *Adv. Protein Chem.* 38: 181–364.

Krimm, S. 1987. Peptides, and Proteins. *In* Biological Applications of Raman Spectroscopy. Spiro, T. G., editor. John Wiley, New York. 3–45.

Murphy, K. P., P. L. Privalov, and S. J. Gill. 1990. Common features of protein unfolding, and dissolution of hyrophobic compounds. *Science.* 247:559–561.

Pease, L. G., and C. Watson. 1978. Conformational, and ion binding studies of a cyclic pentapeptide. Evidence for β, and γ turns in solution. *J. Am. Chem. Soc.* 100:1279–1286.

Raymond, J. A., and A. L. DeVries. 1977. Adsorption inhibition as a mechanism of freezing resistance in polar fishes. *Proc. Natl. Acad. Sci. USA.* 74:2589–2593.

Tomimatsu, Y., J. R. Scherer, Y. Yeh, and R. E. Feeney. 1976. Raman spectra of a solid antifreeze glycoprotein, and its liquid, and frozen aqueous solutions. *J. Biol. Chem.* 251:2290–2297.

Van Wart, H. E., and H. A. Scheraga. 1978. *Methods Enzymol.* 44:124–149.

Vasko, P. D., J. Blackwell, and J. L. Koenig. 1972. Infrared, and Raman spectroscopy of carbohydrates. *Carbohydr. Res.* 23:407–416.

Yang, D. S. C., M. Sax, A. Chakrabartty, and C. L. Hew. 1988. Crystal structure of an antifreeze polypeptide, and its mechanistic implications. *Nature.* 333:232–237.

[3] There is evidence of interaction between the peptide backbone and the disaccharides (Bush, 1984, 1986).